

# THE EFFECTS OF FIBRE ARCHITECTURE ON WATER ABSORPTION INDUCED DEGRADATION IN CFRP LAMINATES

Faisal Almudaihesh<sup>1</sup>, Rhys Pullin<sup>1</sup>, Karen Holford<sup>1</sup>, and Mark Eaton<sup>1</sup>

<sup>1</sup>School of Engineering, Cardiff University, Queen's Buildings, The Parade, Cardiff CF24 3AA, United Kingdom

Email: almudaiheshfs@cardiff.ac.uk

<sup>1</sup>School of Engineering, Cardiff University, Queen's Buildings, The Parade, Cardiff CF24 3AA, United Kingdom

Email: pullinr@cardiff.ac.uk, Web Page: <https://www.cardiff.ac.uk/people/view/364455-pullin-rhys>

<sup>1</sup>School of Engineering, Cardiff University, Queen's Buildings, The Parade, Cardiff CF24 3AA, United Kingdom

Email: holford@cardiff.ac.uk, Web Page: <https://www.cardiff.ac.uk/people/view/364385-holford-karen>

<sup>1</sup>School of Engineering, Cardiff University, Queen's Buildings, The Parade, Cardiff CF24 3AA, United Kingdom

Email: eatonm@cardiff.ac.uk, Web Page: <https://www.cardiff.ac.uk/people/view/364361-eaton-mark>

**Keywords:** Carbon-polymer matrix composites, Fibre architectures, water absorption, moisture damage mechanism, and experimental analysis.

## Abstract

The fibre architecture not only plays a significant role in the mechanical properties and the damage mechanisms of carbon fibre reinforced polymers but also on the water ingress mechanism. Unidirectional and 2D woven CFRP were evaluated after water absorption. Weight gain was monitored along with the evaluation of compressive strength, short-beam strength, and impact damage resistance in water-saturated and dry specimens. Microscopic imaging was used in some of the experimental testing to monitor the performance of dry and water-immersed specimens in terms of damage mechanisms. The results showed higher weight gain levels in unidirectional CFRP in undamaged specimens. However, 2D woven CFRP suffered higher water uptake when they were subjected to impact damage prior to water exposure. Reductions in the mechanical properties were primarily observed for matrix dominated properties for both unidirectional and 2D woven CFRP types.

## 1. Introduction

The use of CFRP laminates are significantly increasing in the aerospace, automotive, and marine industries particularly in safety critical primary structures due to their excellent fatigue and corrosion resistance properties compared with metallic materials [1]. CFRP prepregs consist of reinforcing carbon fibres distributed in an epoxy resin which can be in the form of unidirectional or a range of woven architectures in both biaxial and triaxial forms. Prepregs are particularly attractive due to their precisely controlled resin distribution [2,3]. Many CFRP structures are at high risk of structural and environmental impacts whilst in operation which can significantly influence their overall performance [4]. This study aims to evaluate the influence of the fibre architecture on the water ingress and subsequent degradation of CFRP. The study considers a unidirectional and two 2D woven architectures: plain weave and 2x2 twill weave. Each material is tested under compression, short-beam shear, and impact damage to assess how individual material properties are affected. The aim is to understand the consequences of moisture absorption when using different fibre architecture and provide information that can help to minimise the influence of moisture and reduce the likelihood of unexpected failures in future designs.

## 2. Materials and Experimental Methods

### 2.1 Materials

Three versions of CFRP prepreg were used in this work manufactured by SK chemicals using Skyflex K51 Epoxy resin and Pyrofil TR50S high strength carbon fibres. The specification of each prepreg variant used were: unidirectional, 200gsm with 33% resin content; 3k plain weave, 198gsm with 40% resin content; and 2x2 3k twill weave, 198gsm with 40% resin content. All materials were cured with the same cure cycle as recommended by the materials supplier, using an autoclave under two dwells: 30 minutes at 80°C temperature and 5 bar pressure followed by 60 minutes at 125°C temperature and 5 bar pressure. Large panels were manufactured for each particular test with the required stacking sequences. The specimens were then cut into the desired dimensions, and c-scanned to ensure manufacturing quality. The matrix volume content was obtained for all specimens in accordance with ASTM D3171 method 2 [5].

### 2.2 Water Absorption

Water absorption testing was carried out using non-ambient moisture conditioning in a water immersion tank with demineralised water at a prescribed constant temperature of 70°C for a fixed-time period of 40 days in accordance with ASTM D5229 procedure BWFF [6]. The specimen water content was determined as a percentage change using (Eq. 1) [6]:

$$\text{Mass percentage change, \%} = \left( \frac{W_i - W_o}{W_o} \right) \times 100 \quad (1)$$

Where  $W_i$  is the weight of the specimen at each point of record during the experiment, and  $W_o$  is the initial dry weight of the specimen before any contact with water.

### 2.3 Compressive Strengths

The compressive strengths were obtained using a combined loading compression (CLC) test carried out in accordance to ASTM D 6641 [7]. Ten specimens were prepared for each fibre architecture (five dry and 5 water-immersed) with dimensions of 140mm ( $\pm 0.3$ ) by 13mm with gauge length of 13mm. Sixteen plies were used with stacking sequences of  $[0/90]_{4S}$  and  $[(0/90)]_{16}$  producing thicknesses of 3.06mm, 3.54mm, 3.51 for unidirectional, plain, and twill, respectively. These stacking sequences create an identical distribution of fibre directions between the unidirectional and woven specimens for comparison purposes. A 1 mm thick aluminium caul plate covered with nylon was used inside the vacuum bag in order to achieve a smooth surface on the bag side. This step was essential to achieve the desired surface finish on both sides of the specimens required for CLC fixture. The fibre volume fraction and void content for these specimens are presented in Table 1. An Avery-Denison loading machine with 600kN load cell and two fixed platens was used to apply load to the CLC fixture at a rate of 1.3mm/min. The CLC fixture screws were tightened with a torque of 3.5N-m to hold specimens. The laminate compressive strength was calculated using (Eq. 2) [7]:

$$F_{cu} = \frac{p_f}{w \times h} \quad (2)$$

Where  $F_{cu}$  is laminate compressive strength (MPa),  $p_f$  is the maximum load to failure (N),  $w$  is the measured specimen gage width (mm), and  $h$  is the measured specimen gage thickness (mm).

**Table 1.** Compression specimens

Fibre Architecture	Matrix Volume (%)
Unidirectional	42.68
Plain	50.50
Twill	49.99

## 2.4 Short-beam Strengths

The short-beam strengths were obtained using a three-point bending configuration in Zwick Roell Z050 loading machine with 50kN load cell. The loading nose was 6mm in diameter, the supports were 3mm in diameter, the span distance was 24mm and the speed of testing was at a rate of 1mm/min in accordance with ASTM D2344 [8]. Ten specimens were prepared for each fibre architecture (five dry and 5 water-immersed) with dimensions of 36mm by 12mm. There were thirty plies with stacking sequences of  $[0/90]_{15}$  and  $[(0/90)]_{30}$  for unidirectional (5.73mm thick) and woven (6.9mm thick for plain and 6.42mm for twill), respectively. The stacking sequences were selected to create an identical distribution of fibre directions between unidirectional and woven specimens for comparison purposes. Debulking operations were applied when making the specimens due to their large thicknesses. The debulking process consisted of five minutes vacuum pressure at room temperature for each five plies prior to the main cure cycle [9]. The fibre volume fractions and void content for these specimens are presented in Table 2. The short-beam strength was calculated using (Eq. 3) [8]:

$$F_{sbs} = 0.75 \times \frac{p_m}{b \times h} \quad (3)$$

Where  $F_{sbs}$  is the short beam strength (MPa),  $p_m$  is the maximum load observed during the test (N),  $b$  is the measured specimen width (mm), and  $h$  is the measured specimen thickness (mm).

**Table 2.** Short-beam specimens

Fibre Architecture	Matrix Volume (%)
Unidirectional	41.94
Plain	51.87
Twill	49.06

## 2.5 Impact Damage Resistance

Fifteen specimens were prepared for each fibre architecture in order to investigate the influence of different levels of impact damages on water uptake of each fibre architecture. Artificial damages were applied with a 16mm ( $\pm 0.1$ ) hemispherical striker tip impactor with a mass of 5.5kg ( $\pm 0.25$ ), dropped from different heights to obtain the required energy using an Instron 9250-HV drop tower in accordance with ASTM D 7136 [10]. All specimens were 150mm ( $\pm 0.25$ ) by 100mm ( $\pm 0.25$ ) with stacking sequences of  $[45/0/-45/90]_{3s}$  for unidirectional and  $[(45/-45)/(0/90)]_{6s}$  for woven resulting in thicknesses of 4.55mm, 4.8mm, and 4.9mm for unidirectional, plain, and twill, respectively. Perforated release film and double breather fabric were used in the vacuum bag in order to allow easier bleed of resin from the bag side due to the size of the panels which were significantly larger than those in previous studies. The fibre volume fractions and void content for these specimens are presented in Table 3. Prior to the water absorption experiment, 10 specimens of each fibre architecture were impacted, five with an energy of 20J, and 5 with an energy of 70J to represent barely visible impact damage (BVID), and visible impact damage (VID), respectively. The five remaining specimens were left undamaged for comparison with water uptake of undamaged specimens. The undamaged specimens were then impacted with 70J following the water immersion testing, in order to investigate the influence of moisture absorption on impact resistance.

**Table 3.** Impact damage resistance specimens

Fibre Architecture	Matrix Volume (%)
Unidirectional	41.70
Plain	44.66
Twill	45.99

## 2.6 Microscopic Imaging and C-scanning

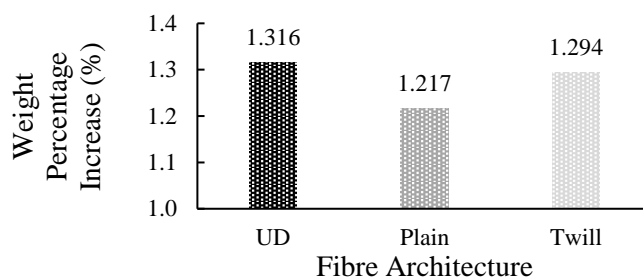
An Olympus B07 microscope with a Moticam 10.0 MP camera was used to acquire images. The images were then post processed using Motic Images Plus 2.0 ML to insert dimensions and trim images to the area of interest for the analysis of damage mechanism of different specimens. For internal assessment of internal damage, a submersion tank ultrasonic c-scanning system supplied by MIDAS NDT Systems Ltd. was used. The scan was operated in pulse-receive mode using a 10MHz probe. The data were then post processed using ZEUS V3 software.

## 3. Results and Discussions

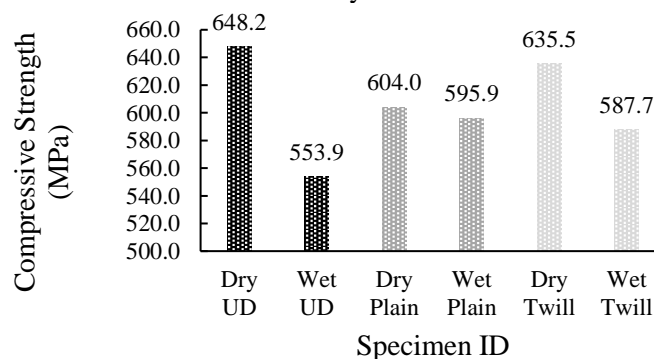
### 3.1 Water Absorption vs Compressive Strength

Fig. 1 shows the average weight increase for compression specimens prior to compressive testing and Fig. 2 presents the average compressive strength obtained for all specimens. Reductions in the compressive strengths were noted for all wet specimens, the extent of which is well correlated to the percentage moisture uptake. This results from plasticisation of the polymeric matrix promoted by the water absorption, particularly in the interfacial region which is critical for compressive properties [11]. The plasticisation causes a reduction in stiffness and yield strength of the matrix therefore offering less support to the load bearing fibres hence the observed reduction in composite strength. Plasticisation also increases ductility and toughness of the matrix which has led to a change in the observed failure mechanisms with much less interlaminar cracking present.

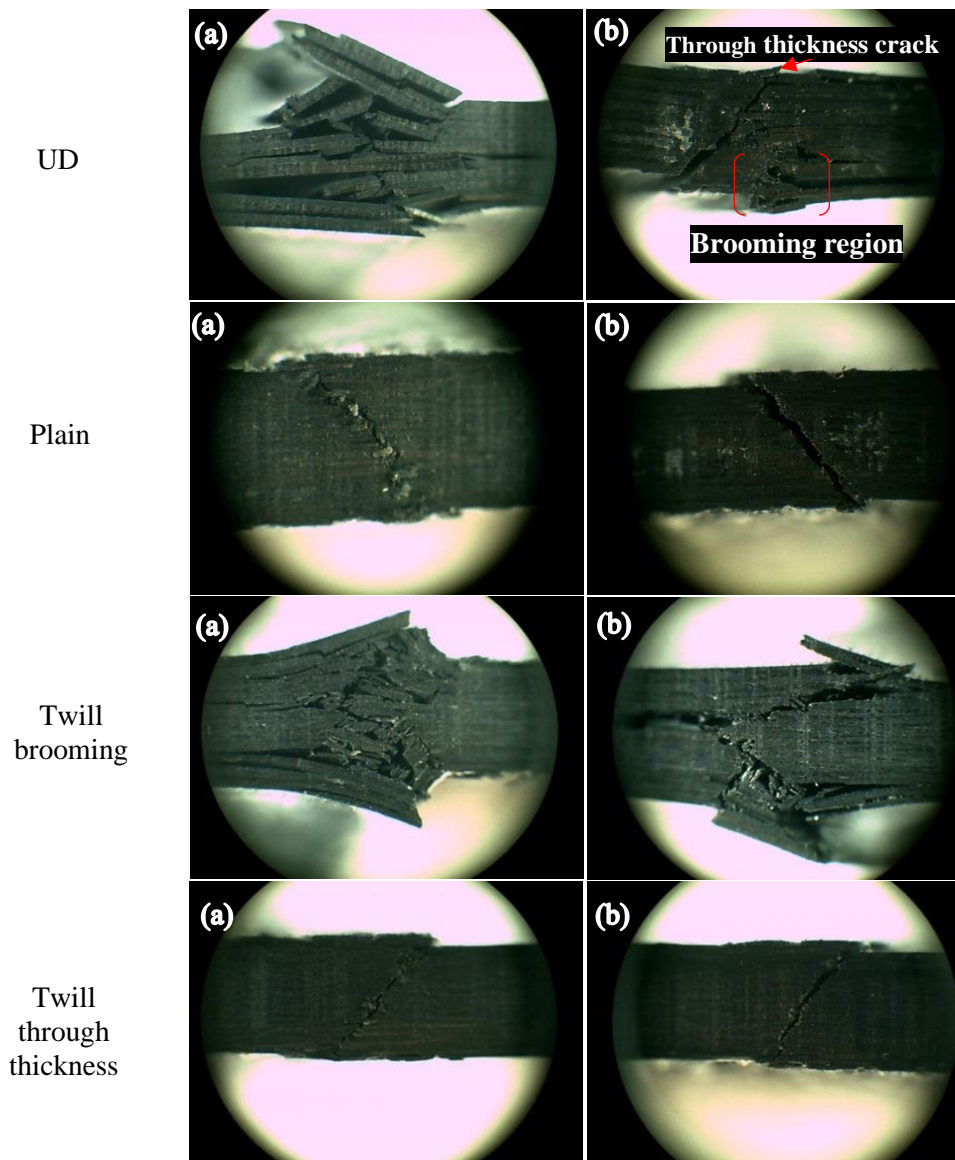
In the case of the UD specimens mostly brooming in the gage area, with significant interlaminar cracking is seen for dry specimens, whereas most wet UD specimens suffered less brooming (hence less interlaminar cracking) and more through thickness cracks appearing (Fig. 3). For plain weave specimens, through thickness cracking at the grip was recorded for most dry and wet specimens (Fig. 3). For twill specimens, two failure modes were observed in both dry and wet specimens which were brooming in the gage area and through thickness cracking at the grip. In the regions of through thickness cracking (all specimen types) less interlaminar micro-cracks are observed for the wet specimens further demonstrating the increased ductility and toughness caused by plasticisation. It is worth noting that all failure modes obtained are in agreement with acceptable failure modes reported in ASTM D 6641 [7].



**Figure 1.** Average weight gain for unidirectional, plain, and twill specimens for compressive strength analysis



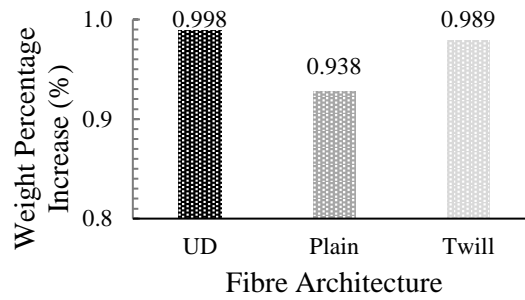
**Figure 2.** Average laminate maximum compressive strengths for dry and water-immersed unidirectional, plain, and twill CFRP specimens.



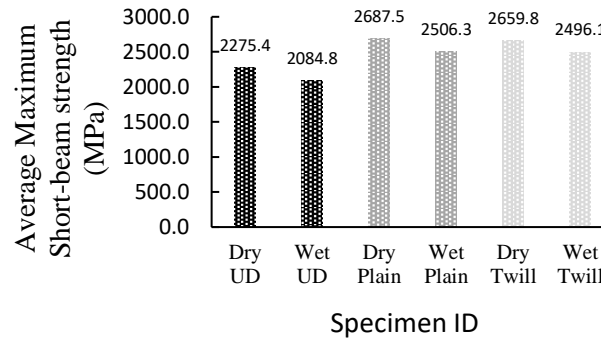
**Figure 3.** Digital microscopy images of failure modes for compression specimens for UD, plain, and twill (a) dry and (b) water-immersed.

### 3.2 Water Absorption vs Short-beam strength

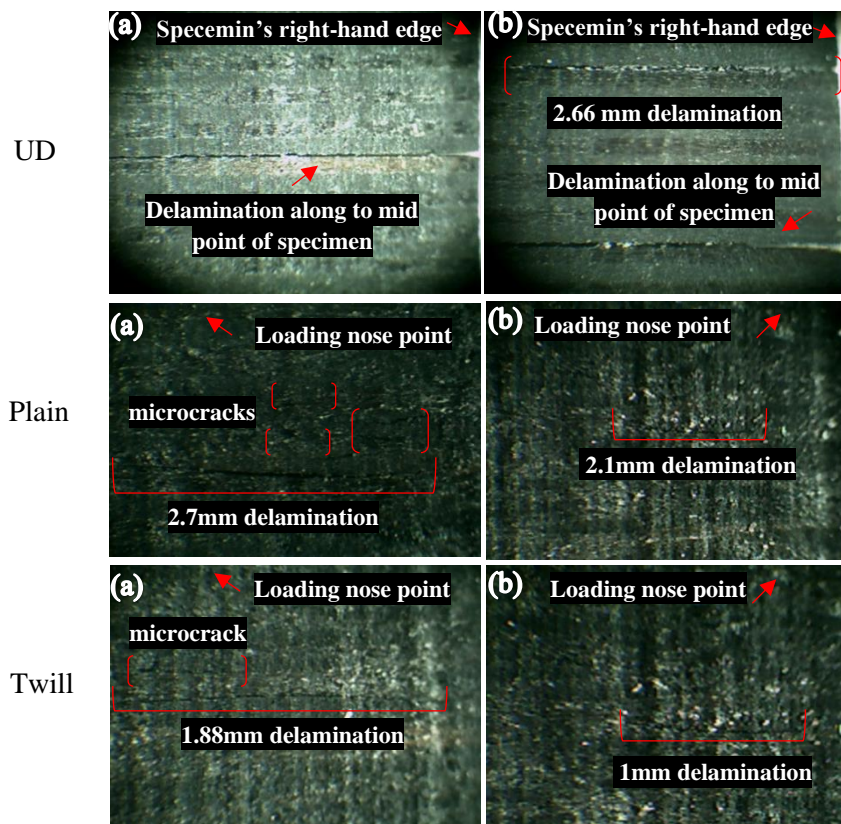
Similar trends to that of the compressive strength specimens were obtained for short-beam specimens in terms of weight gain as presented in Fig 4 where UD specimens averaged higher uptake than that of the woven specimens. Fig. 5 presents the average short-beam strengths for all specimens. A single delamination along the longitudinal axis was observed for all UD specimens, with more than one delamination observed in wet UD specimen. It is believed that the increase in crack density due to water exposure in UD specimens have promoted degradation in the interlaminar regions allowing the several longitudinal cracks observed in wet specimens as presented in Fig. 6. A similar observation was reported by Barbosa et al when studying the influence of accelerated aging on carbon/epoxy composites [12]. For woven architectures, the main failure mode obtained for all dry and wet specimens was reported as delamination near the compression region with smaller delamination lengths and fewer microcracks in wet specimens. A potential cause is that the affected matrix has diffused less stress within the fibres crossover points/crimp regions in wet specimens leading the material to resist lower loads (subsequently, smaller cracks observed) in fewer regions (subsequently, lower microcracks observed).



**Figure 4.** Weight gain for unidirectional, plain, and twill specimens for short-beam strength analysis.



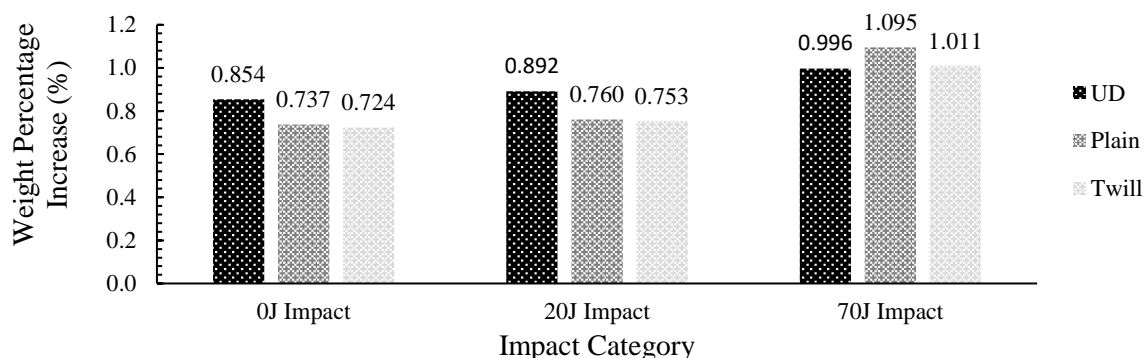
**Figure 5.** Average short-beam strengths for dry and water-immersed unidirectional, plain, and twill CFRP specimens



**Figure 6.** Digital microscopy images of short-beam specimens after failure (a) dry and (b) water-immersed.

### 3.3 Water Absorption vs Impact Damage Resistance

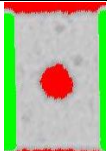
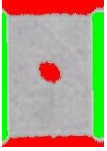
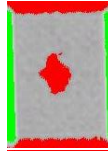
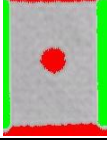
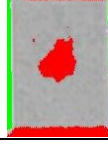
The average weight gains for all impact damage specimens are summarised in Fig. 7. In line with the compression and short-beam specimens, the undamaged UD specimens exhibit higher average weight gain than that observed in the woven specimens. Moisture absorption increased with increasing impact energy in all specimens and significant increases were seen at high impact energies (70J). At the 70J impact energy, it was also observed that the moisture uptake of the woven samples now exceeded that



**Figure 7:** Average weight gain for impact damage resistance specimens categories.

of UD specimens. This results from a greater extent of surface damage and through thickness damage observed in the woven specimens, as reported in other studies [13,14], which allows easier moisture ingress into a large volume of damage for these specimens. The specimens impacted at 70J after moisture absorption exhibited similar trends in observed surface damage and minimal changes in delamination size measured from C-Scan data presented in Table. 4, with only the UD specimens exhibiting a small increase in delamination size. This is in line with the larger reduction in short-beam strength observed after moisture absorption for the UD specimens above. This shows that matrix degradation is playing a larger role in the impact resistance of UD laminates compared with their woven equivalents.

**Table 4.** The average extent of internal damage diameter (mm) measured in accordance with ASTM D 7136 [10].

Fibre Architecture	20J Impact	70J Impact	70J Impact after water immersion
UD	 32.8 ±0.2	 68.4 ±0.2	 72.8 ±0.2
Plain	 19.2 ±0.2	 26.8 ±0.2	 26.0 ±0.2
Twill	 20.4 ±0.2	 25.6 ±0.2	 24.4 ±0.2

### 4. Conclusions

It was observed that the layout for fibres has influenced the water absorption rates within the CFRP components where water uptake levels were noted for different fibre architectures with higher rates observed for all UD specimens. Reductions in the mechanical properties were reported in all water-

immersed specimens due to polymer degradation promoted by the water ingress, with higher moisture uptake correlating to larger reductions in strength. 2D woven fibre architectures suffered greater moisture absorption following impacts at high energies (70J) prior to water exposure. It was also noted that the specimen's geometry, bagging procedure for manufacturing, and stacking sequences have also influenced the rate of water absorption within the structure. Thus, further research on the influence of the manufacturing process and fibres layout in terms of their stacking sequences on the water penetration of CFRP is desired.

## References

- [1] Takeda SI, Tsukada T, Sugimoto S, Iwahori Y. Monitoring of water absorption in CFRP laminates using embedded fiber Bragg grating sensors. *Compos Part A Appl Sci Manuf* 2014;61:163–71. doi:10.1016/j.compositesa.2014.02.018.
- [2] Xu L, Huang Y, Zhao C, Ha SK. Progressive failure prediction of woven fabric composites using a multi-scale approach. *Int J Damage Mech* 2018;27:97–119.
- [3] Meredith J, Bilson E, Powe R, Collings E, Kirwan K. A performance versus cost analysis of prepreg carbon fibre epoxy energy absorption structures. *Compos Struct* 2015;124:206–13.
- [4] Baley C, Davies P, Grohens Y, Dolto G. Application of Interlaminar Tests to Marine Composites. A Literature Review. *Appl Compos Mater* 2004;11:99–126. doi:10.1023/B:ACMA.0000012902.93986.bf.
- [5] ASTM D3171. Standard Test Methods for Constituent Content of Composite Materials. Am Soc Test Mater 2015.
- [6] ASTM D 5229. Standard Test Method for Moisture Absorption Properties and Equilibrium Conditioning of Polymer Matrix Composite Materials. Am Soc Test Mater 2014.
- [7] ASTM D 6641. Standard Test Method for Compressive Properties of Polymer Matrix Composite Materials Using a Combined Loading Compression (CLC) Test Fixture. Am Soc Test Mater 2009.
- [8] ASTM D2344. Standard Test Method for Short-Beam Strength of Polymer Matrix Composite Materials and Their Laminates. Am Soc Test Mater 2016.
- [9] Campbell FC. *Manufacturing Processes for Advanced Composites*. Oxford: Elsevier Advanced Technology; 2004.
- [10] ASTM D7136. Standard Test Method for Measuring the Damage Resistance of a Fiber-Reinforced Polymer Matrix Composite to a Drop-Weight Impact Event. Am Soc Test Mater 2015.
- [11] Martin K. *Analysis of Failure in Fibre Polymer Laminates The theory of Alfred Puck*. New York: Springer; 2008.
- [12] Cysne Barbosa AP, Ana AP, S.S. Guerra E, K. Arakaki F, Tosatto M, Maria MC, et al. Accelerated aging effects on carbon fiber/epoxy composites. *Compos Part B Eng* 2017;110:298–306.
- [13] Giannopoulos IK, Theotokoglou EE, Zhang X. Impact damage and CAI strength of a woven CFRP material with fire retardant properties. *Compos Part B Eng* 2016;91:8–17.
- [14] Liu H, Falzon BG, Tan W. Predicting the Compression-After-Impact (CAI) strength of damage-tolerant hybrid unidirectional/woven carbon-fibre reinforced composite laminates. *Compos Part A Appl Sci Manuf* 2018;105:189–202.